17th AIAA/CEAS Aeroacoustics Conference, 6–8 June 2011, Portland, Oregon, USA

The critical layer in sheared flow

E.J. Brambley*
DAMTP, University of Cambridge, UK
M. Darau† and S.W. Rienstra‡
Dept. of Maths and Comp. Science, TU Eindhoven, Netherlands

Critical layers arise as a singularity of the linearized Euler equations when the phase speed of the disturbance is equal to the mean flow velocity. They are usually ignored when estimating the sound field, with their contribution assumed to be negligible. It is the aim of this paper to study fully both numerically and analytically a simple yet typical sheared ducted flow in order to distinguish between situations when the critical layer may or may not be ignored. The model is that of a linear-then-constant velocity profile with uniform density in a cylindrical duct, allowing for exact Green's function solutions in terms of Bessel functions and Frobenius expansions. It is found that the critical layer contribution decays algebraically in the constant flow part, with an additional contribution of constant amplitude when the source is in the boundary layer, an additional contribution of constant amplitude is excited, representing the hydrodynamic trailing vorticity of the source. This immediately triggers, for thin boundary layers, the inherent convective instability in the flow. Extra care is required for high frequencies as the critical layer can be neglected only together with the pole beneath it. For low frequencies this pole is trapped in the critical layer branch cut.

I. Introduction

Critical layers arise in inviscid shear flows as a mathematical singularity of the linearized Euler equations at points where the phase velocity is equal to the local fluid velocity, and give rise to a branch point of a complex logarithm in the solution. This can be smoothed out by taking into account additional viscous or nonlinear terms in the neighborhood of the singular point (see [1–3]). However, one can avoid adding complexity to the problem by defining a proper branch cut for the complex logarithm [4] based on causality arguments, with the restriction that the Fourier inversion contour in the wavenumber plane should not cross the branch cut.

Critical layer singularities are associated with the continuous (hydrodynamic) spectrum [5, 6], and have so far been proved to have an algebraic rather than exponential decay or growth rate, as is the case for swirling flows [7–9].

The reference paper for critical layers in a duct carrying sheared flow has so far been the one by Swinbanks [10] in 1975. Considering the sound field in a duct carrying sheared flow with arbitrary Dirichlet-Neumann boundary conditions, he found that the eigenfunction representation of the pressure field generated by a mass source breaks down at the critical layer. Thus, the normal modes no longer form a complete basis, and one has to also add a contribution from the continuous spectrum. This latter part is only present downstream. In the case of a hard-walled duct with a constant velocity profile except for a thin boundary layer,

*Research Fellow, Department of Applied Mathematics & Theoretical Physics, University of Cambridge, CMS, Wilberforce Road, Cambridge, CB3 0WA, United Kingdom, AIAA member
†PhD Student, jointly Department of Mathematics and Computer Science, Eindhoven University of Technology, P.O. Box 513, 5600 MB Eindhoven, The Netherlands, and Faculty of Mathematics and Computer Science, West University of Timişoara, 4 Vasile Parvan Avenue, Timişoara 300223, Romania.
‡Associate Professor, Department of Mathematics and Computer Science, Eindhoven University of Technology, P.O. Box 513, 5600 MB Eindhoven, The Netherlands, Senior Member AIAA

this contribution comes in, in the worst case scenario when the source is at the critical layer, as a singularity consisting of a simple pole and a logarithmic branch point. Inverting the Fourier transform [11] results in an algebraic decay (as $1/x^3$ for a point mass source, and as $1/x^{1/2}$ for a source of distributed nature). This was recently proved for a numerical solution by Felix and Pagneux [12] (still for hard-walled ducts only).

When it comes to determine the sound field in a lined duct, the critical layer is either explicitly [13] or tacitly [14] ignored in the majority of the cases, assuming its contribution to the total field to be insignificant. Numerical methods detect the critical layer as a set of spurious eigenvalues clustered on the positive real wavenumber axis [15, 16]. It is our purpose here to investigate the effects of the critical layer for a simple model having as few parameters as possible (see Eq. (2)), and understand the effects linked to it, as well as its various contributions to the total field.

The paper is a study of the field generated by a time-harmonic point mass source in a circular duct with a constant-then-linear mean flow and a constant density profile. This choice is justified in the beginning of section II as the simplest possible scenario where a critical layer singularity occurs. Solutions to the Pridmore-Brown equation are given in terms of Bessel functions for the constant flow and Frobenius series for the constant shear, thus having the necessary tools for constructing the Green's function for a point mass source. When the source is located in the constant flow part, the Green's function has an equivalent expression to the one for uniform flow [17], as expected. In Section III we analyse the contributions from the poles, finding for the case when the source is at the critical layer (in the boundary layer) an additional pole on the branch cut [10] with a contribution of constant amplitude. This analysis is then illustrated in section IV with a collection of numerical examples, demonstrating the field of the pole on the branch cut and a comparison with the uniform flow case. We also show here the effects of two additional poles linked to the critical layer, one that always has to be considered together with the branch cut, and another weak convective instability. Motivated by these numerical results, we prove in section V that in the far x field the branch cut integral is algebraically decaying as $1/x^4$. Finally, the essentially hydrodynamic nature of the pole on the branch cut is proved in section VI by taking the incompressible limit, showing that its field is the trailing vorticity of the source. A thorough explanation of the effects coming from the choice of source is given in Appendix A.

II. Formulation of the mathematical problem

A. Existence of critical layer singularities

Time-harmonic acoustic perturbations of frequency ω in sheared flow can be found by Fourier series expansion in the circumferential coordinate θ and Fourier transformation to the axial coordinate x with wave number k. The resulting equation to be solved is known as the Pridmore-Brown equation [18]

$$\tilde{p}'' + \Big(\frac{2kU'}{\omega - kU} + \frac{1}{r} - \frac{\rho_0'}{\rho_0}\Big)\tilde{p}' + \Big(\frac{(\omega - kU)^2}{c_0^2} - k^2 - \frac{m^2}{r^2}\Big)\tilde{p} = 0, \tag{1}$$

where the mean velocity and density are $U(r)$ and $\rho_0(r)$ and the square of the speed of sound is $c_0^2 = \gamma p_0/\rho_0$. For suitable solutions $\tilde{p} = p_m(r,k)$ and amplitudes $A_m(k)$ the physical pressure field is given by the (real part of the) sum over Fourier integrals

$$\mathrm{e}^{\mathrm{i}\omega t} \sum_{m=-\infty}^{\infty} \mathrm{e}^{-\mathrm{i}m\theta} \int_{-\infty}^{\infty} A_m(k) p_m(r,k)\, \mathrm{e}^{-\mathrm{i}kx}\, \mathrm{d}k.$$

Well-chosen indentations of the k-inversion contour are understood when singularities of any kind along the real axis are to be avoided. In this paper we will be interested in a single m-mode, represented by the k-integral, for the field of a point source.

Equation (1) contains a regular singularity at $r = r_c$, where $\omega - kU(r_c) = 0$. This singularity is referred to as a critical layer, and leads to a continuous hydrodynamic spectrum. Two linearly independent solutions for $\tilde{p}$ expanded about r_c are

$$\begin{aligned}
&\tilde{p}_1(r) = (r - r_c)^3 + O((r - r_c)^4),\\
&\tilde{p}_2(r) = A\tilde{p}_1(r)\log(r - r_c) + 1 - \tfrac{1}{2}(k^2 + m^2/r_c^2)(r - r_c)^2 + O((r - r_c)^4),
\end{aligned}$$

where

$$A = -\frac{1}{3}\left(k^2 + \frac{m^2}{r_c^2}\right)\left(\frac{U''(r_c)}{U'(r_c)} + \frac{\rho_0'(r_c)}{\rho_0(r_c)} - \frac{1}{r_c}\right) - \frac{2m^2}{3r_c^3}. \tag{2}$$

The log-singularity is removed when the coefficient A is zero. In general, A will be nonzero, even for planar shear (rather than, as is considered here, cylindrical shear) where the $1/r_c$ term in (2) is not present. The notable case when A is identically zero is for linear planar shear of a uniform density fluid. In other words, unless the shear is planar, the density is uniform, and the velocity is either constant or linear, then the log-singularity will in general be present. A relation similar to (2) regarding the existence of the critical layer is mentioned in Ref. [19] for uniform density.

B. Solutions to the Pridmore-Brown equation

Here, we consider a linear shear with constant density in a cylindrical duct, and scale distances on the duct radius a, velocities on the sound speed c_0, density on the mean density ρ_0, pressure on $\rho_0 c_0^2$ and impedance on $\rho_0 c_0$, thus having the duct wall at $r = 1$ and

$$U(r) = \begin{cases} M, & 0 \leqslant r \leqslant 1-h, \\ M(1-r)/h, & 1-h \leqslant r \leqslant 1, \end{cases}$$

with M the mean flow Mach number. Hence, equation (1) becomes

$$p'' + \Big(\frac{2kU'}{\omega - kU} + \frac{1}{r}\Big)p' + \Big((\omega - kU)^2 - k^2 - \frac{m^2}{r^2}\Big)p = 0. \tag{3}$$

1. *Solution within the constant-flow region*

The solutions to Eq. (3) are given within the uniform-flow section $r < 1-h$ by

$$p = A\mathrm{J}_m(\alpha r) + B\mathrm{Y}_m(\alpha r) \qquad \text{or equivalently} \qquad p = C_1\mathrm{H}_m^{(1)}(\alpha r) + C_2\mathrm{H}_m^{(2)}(\alpha r),$$

where $\alpha^2 = (\omega - Mk)^2 - k^2$. Since $\mathrm{Y}_m(z)$, $\mathrm{H}_m^{(1)}(z)$ and $\mathrm{H}_m^{(2)}(z)$ contain log-like singularities, a branch cut needs to be chosen for α, which (for fixed ω) leads to two branch cuts in the k-plane. Branch cuts of Bessel functions are traditionally taken along the negative real z axis, although they could be taken anywhere using analytic continuation. However, the traditional branch cuts will be fine provided the branch cut chosen for α means that αr is never real and negative. Taking branch cuts along $\alpha^2 = \mathrm{i}q$ for $q \in \mathbb{R}^+$ gives the additional desirable property that no branch cut crosses the imaginary k axis for ω having a negative imaginary part (see Figure 1*a*). For $x < 0$, the k inversion contour needs to be closed in the upper half plane, giving an inversion contour $\mathcal{C}_- \cup \mathcal{C}_-'$ shown in figure 1*b*, with $\mathcal{C}_-$ being the contribution from the poles in the upper-half plane and $\mathcal{C}_-'$ being the contribution from the α branch cut. For $x > 0$, the k inversion contour similarly needs to be taken as $\mathcal{C}_+ \cup \mathcal{C}_+' \cup \mathcal{C}_+''$.

However, the branch cuts in the α^2 plane are removable, at least as far as the Green's function is concerned. This is because crossing a branch cut sends $\mathrm{J}_m(\alpha r)$ to $\mathrm{J}_m(-\alpha r) = (-1)^m \mathrm{J}_m(\alpha r)$, and $Y_m(\alpha r)$ to $\mathrm{Y}_m(-\alpha r) = A\mathrm{J}_m(\alpha r) + B\mathrm{Y}_m(\alpha r)$, where A and B are constants independent of α or r (see Abramowitz & Stegun [20, p.361]). Therefore, if we are interested in the function $f(r) = C\mathrm{J}_m(\alpha r) + D\mathrm{Y}_m(\alpha r)$, where constants C and D have been chosen so that $f(r_1)$ and $f'(r_1)$ take known values, then the function $f(r)$ will be identical on either side of the branch cut. The integrals around the $\mathcal{C}_+'$ and $\mathcal{C}_-'$ contours are therefore identically zero, and so these branch cuts may be ignored.

2. *Frobenius expansion for constant shear*

For $1-h < r < 1$, the mean flow becomes $U(r) = M(1-r)/h$ and the Pridmore-Brown equation is singular at $r = r_c$, where $r_c = 1 - \omega h/(kM)$ (possibly complex). Substituting $R = r - r_c$ into Eq. (3) for this constant shear gives

$$p_{RR} + \left(\frac{1}{r_c + R} - \frac{2}{R}\right)p_R + \left(\eta^2 R^2 - k^2 - \frac{m^2}{(R + r_c)^2}\right)p = 0,$$

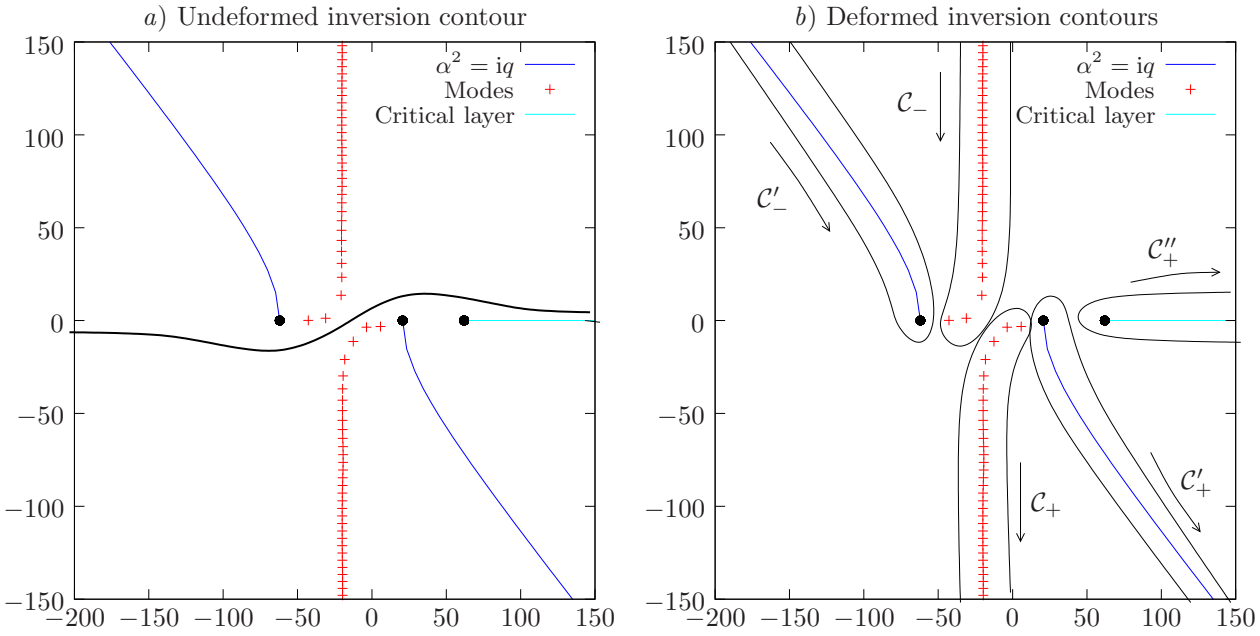

Figure 1. Schematic of the complex k plane, including branch cuts of α, the critical layer, modes, and integration contours. *a*) The undeformed causal inversion contour. *b*) The inversion contour deformed for $x < 0$ ($\mathcal{C}_-$ and $\mathcal{C}'_-$) and $x > 0$ ($\mathcal{C}_+$, $\mathcal{C}'_+$ and $\mathcal{C}''_+$).

where a subscript R denotes $\mathrm{d}/\mathrm{d}R$ and $\eta = Mk/h$. We pose a Frobenius expansion about this singularity, leading to the two linearly independent solutions:

$$p_1(r) = \sum_{n=0}^{\infty} a_n (r - r_c)^{n+3}, \qquad p_2(r) = \frac{1}{3r_c}\left(k^2 - \frac{m^2}{{r_c}^2}\right) p_1(r) \log(r - r_c) + \sum_{n=0}^{\infty} b_n (r - r_c)^n, \tag{4a}$$

$$a_n = \frac{1}{n(n+3)}\left[k^2 a_{n-2} - \eta^2 a_{n-4} - \sum_{q=0}^{n-1} a_{n-1-q}(-1)^q \big(n + 2 + (m^2 - 1)q\big)/{r_c}^{q+1}\right], \tag{4b}$$

$$\begin{aligned} b_n = \frac{1}{n(n-3)}\Bigg[&k^2 b_{n-2} - \eta^2 b_{n-4} - \sum_{q=0}^{n-1} b_{n-1-q}(-1)^q \big(n - 1 + (m^2 - 1)q\big)/{r_c}^{q+1} \\ &- \frac{1}{3r_c}\left(k^2 - \frac{m^2}{{r_c}^2}\right)\left((2n-3)a_{n-3} + \sum_{q=0}^{n-4} a_{n-4-q}(-1)^q/{r_c}^{q+1}\right)\Bigg], \end{aligned} \tag{4c}$$

$$a_n = b_n = 0, \text{ for } n < 0; \quad a_0 = b_0 = 1; \quad b_3 = 0.$$

The branch cut for the log term in (4a) is taken away from the real r axis, so that $p_2(r)$ is a regular function of r for the physically relevant range $r \in [0, 1]$. For varying k, the direction of this branch cut therefore changes when the branch point at r_c crosses the interval $[0, 1]$ of the real r axis, leading to a branch cut in the k plane on the real k axis for $k \in [\omega/M, \infty)$. It is this k branch cut that is referred to as the *critical layer*. For k below the critical layer branch cut, $\mathrm{Im}(r_c) < 0$, and for k above the critical layer branch cut, $\mathrm{Im}(r_c) > 0$. The change in $p_2(r)$ for k crossing the critical layer branch cut from below is therefore

$$\Delta p_2(r) = \begin{cases} -\dfrac{2\pi \mathrm{i}}{3r_c}\left(k^2 - \dfrac{m^2}{{r_c}^2}\right) p_1(r), & r < \mathrm{Re}(r_c) \\ 0, & r > \mathrm{Re}(r_c), \end{cases}$$

while $p_1(r)$ remains continuous. We will also, on occasion, use the notation $p_2^{\pm}(r)$ to denote the solution $p_2(r)$ with the branch cut taken in the positive (+) or negative (−) imaginary r directions, as these will be useful for analytic continuation.

C. Green's function solution

Green's function solutions capture all possible physics of the problem, since any arbitrary driving disturbance or initial condition can be applied using them. In this paper we are only concerned with the point mass source Green's function (see also Appendix A for the relevance of choosing a mass source, rather than, for example, a point force). Nonetheless, the results we obtain using this Green's function should be seen as, in some sense, general.

The field generated by a point mass source of strength $S = 1$ located at $(x, \theta, r) = (0, 0, r_0)$ is given by

$$G'' + \left(\frac{1}{r} + \frac{2kU'}{\omega - Uk}\right)G' + \left((\omega - Uk)^2 - k^2 - \frac{m^2}{r^2}\right)G = -\mathrm{i}(\omega - U(r_0)k)\frac{\delta(r - r_0)}{2\pi r_0},$$

with the Green's function solution

$$G = \frac{-\mathrm{i}(\omega - U(r_0)k)}{2\pi r_0 W(r_0; \psi_1, \psi_2)}\psi_1(r_<)\psi_2(r_>), \tag{5}$$

where $W = \psi_1\psi_2' - \psi_1'\psi_2$, $r_< = \min\{r, r_0\}$, and $r_> = \max\{r, r_0\}$. The function ψ_1 is the solution to the homogeneous Pridmore-Brown equation (3) satisfying $\psi_1(0) = 0$ for $m \neq 0$ and $\psi_1'(0) = 0$ for $m = 0$. The function ψ_2 is a solution of the same equation, satisfying the impedance boundary condition

$$\mathrm{i}ZG' - \omega G = 0 \qquad \text{at} \qquad r = 1.$$

Both ψ_1 and ψ_2 are required to be C^1 continuous at $r = 1 - h$. We take,

$$\psi_1 = \begin{cases} \mathrm{J}_m(\alpha r) & r \leqslant 1 - h, \\ C_1 p_1(r) + D_1 p_2(r) & r \geqslant 1 - h, \end{cases} \tag{6a}$$

$$\psi_2 = \begin{cases} A_2 \mathrm{H}_m^{(1)}(\alpha r) + B_2 \mathrm{H}_m^{(2)}(\alpha r) & r \leqslant 1 - h, \\ C_2 p_1(r) + D_2 p_2(r) & r \geqslant 1 - h, \end{cases} \tag{6b}$$

where A_2, B_2, C_1 and D_1 are chosen to give C^1 continuity at $r = 1 - h$, and C_2 and D_2 are chosen to satisfy the boundary conditions at $r = 1$, which for definiteness we take to be $\psi_2(1) = 1$ and $\psi_2'(1) = -\mathrm{i}\omega/Z$. This eventually leads to

$$C_1 = \left.\frac{\mathrm{J}_m(\alpha r)p_2' - \alpha \mathrm{J}_m'(\alpha r)p_2}{\widetilde{W}}\right|_{r=1-h} \qquad C_2 = \left.\frac{p_2' + \frac{\mathrm{i}\omega}{Z}p_2}{\widetilde{W}}\right|_{r=1} \tag{7a}$$

$$D_1 = -\left.\frac{\mathrm{J}_m(\alpha r)p_1' - \alpha \mathrm{J}_m'(\alpha r)p_1}{\widetilde{W}}\right|_{r=1-h} \qquad D_2 = -\left.\frac{p_1' + \frac{\mathrm{i}\omega}{Z}p_1}{\widetilde{W}}\right|_{r=1} \tag{7b}$$

$$\begin{pmatrix} A_2 \\ B_2 \end{pmatrix} = \frac{\mathrm{i}\pi(1-h)}{4\widetilde{W}(1)} \begin{pmatrix} \alpha \mathrm{H}_m^{(2)\prime} & -\mathrm{H}_m^{(2)} \\ -\alpha \mathrm{H}_m^{(1)\prime} & \mathrm{H}_m^{(1)} \end{pmatrix}_{r=1-h} \begin{pmatrix} p_1 & p_2 \\ p_1' & p_2' \end{pmatrix}_{r=1-h} \begin{pmatrix} p_2' & -p_2 \\ -p_1' & p_1 \end{pmatrix}_{r=1} \begin{pmatrix} 1 \\ -\mathrm{i}\omega/Z \end{pmatrix}, \tag{7c}$$

where $\widetilde{W}(r) = p_1(r)p_2'(r) - p_1'(r)p_2(r)$, and we have used the identity $W\left(\mathrm{H}_m^{(1)}(\alpha r), \mathrm{H}_m^{(2)}(\alpha r)\right) = -4\mathrm{i}/(\pi r)$ from Abramowitz & Stegun [20] for the final line. The function $\widetilde{W}(r)$ may be calculated directly by substituting into (1), to give

$$\widetilde{W}' + \left(\frac{1}{r} + \frac{2kU'}{\omega - Uk}\right)\widetilde{W} = 0, \qquad \Rightarrow \qquad \widetilde{W} = \widetilde{W}_0 \frac{(\omega - Uk)^2}{r},$$

where $\widetilde{W}_0$ is a constant. From the normalization of p_1 and p_2 used in (4a,b), the constant $\widetilde{W}_0$ may be determined by considering the limit $r \to r_c$, giving

$$\widetilde{W}_0 = \frac{-3r_c h^2}{{U_0}^2 k^2} \qquad \Rightarrow \qquad \widetilde{W}(r) = -3\frac{r_c}{r}(r - r_c)^2. \tag{8}$$

We now consider the two cases $r_0 < 1 - h$ and $r_0 > 1 - h$ separately, before ultimately combining them.

1. Green's function for $r_0 < 1-h$

In this case, the source is in the constant flow region, so that $\psi_1(r_0)$ and $\psi_2(r_0)$ are given in terms of Bessel functions by (6a) and (6b). Expanding $W(r_0;\psi_1,\psi_2)$ in (5) in this case and making further use Bessel function identities from Ref. 20, we finally arrive at

$$G = \frac{-\mathrm{i}(\omega - U_0 k)\widetilde{W}(1)}{2\pi(1-h)Q}\psi_1(r_<)\psi_2(r_>),$$

where $Q = \widetilde{W}(1-h)\widetilde{W}(1)\big(C_1D_2 - C_2D_1\big)$, so that

$$\begin{aligned} Q = \quad & \big(\mathrm{J}_m(\alpha r)p_1' - \alpha \mathrm{J}_m'(\alpha r)p_1\big)\Big|_{r=1-h}\Big(p_2' + \frac{\mathrm{i}\omega}{Z}p_2\Big)\Big|_{r=1} \\ & - \big(\mathrm{J}_m(\alpha r)p_2' - \alpha \mathrm{J}_m'(\alpha r)p_2\big)\Big|_{r=1-h}\Big(p_1' + \frac{\mathrm{i}\omega}{Z}p_1\Big)\Big|_{r=1}. \end{aligned} \tag{9}$$

We note that outside the boundary layer (for $r < 1-h$) this may be written as

$$\begin{aligned} G(r) &= -\tfrac{1}{4}\mathrm{i}(\omega - kM)J_m(\alpha r_<)\left[Y_m(\alpha r_>) - \frac{Y_m(\alpha(1-h)) - Z_1\alpha Y_m'(\alpha(1-h))}{J_m(\alpha(1-h)) - Z_1\alpha J_m'(\alpha(1-h))}J_m(\alpha r_>)\right], \\ Z_1 &= \frac{\big[p_2'(1) + \frac{\mathrm{i}\omega}{Z}p_2(1)\big]p_1(1-h) - \big[p_1'(1) + \frac{\mathrm{i}\omega}{Z}p_1(1)\big]p_2(1-h)}{\big[p_2'(1) + \frac{\mathrm{i}\omega}{Z}p_2(1)\big]p_1'(1-h) - \big[p_1'(1) + \frac{\mathrm{i}\omega}{Z}p_1(1)\big]p_2'(1-h)}, \end{aligned} \tag{10}$$

and we observe that by setting $h = 0$ we recover the Green's function for uniform flow from Ref. [17].

2. Green's function for $r_0 > 1-h$

If $r_0 > 1-h$, the Green's function source is located within the boundary layer. In this case, the Green's function is given by (5), with $W(r_0;\psi_1,\psi_2) = (C_1D_2 - C_2D_1)\widetilde{W}(r_0)$. Using (7a), (7b) and (8) gives

$$G = \frac{-\mathrm{i}(\omega - U(r_0)k)}{2\pi r_0}\frac{\widetilde{W}(1)\widetilde{W}(1-h)}{\widetilde{W}(r_0)Q}\psi_1(r_<)\psi_2(r_>),$$

with Q as defined in (9).

3. Greens function for arbitrary r_0

Note that the previous two sections' results for $r_0 > 1-h$ and $r_0 < 1-h$ may be combined by defining $r^* = \max\{r_0, 1-h\}$ and setting

$$G = \frac{\omega - U(r^*)k}{2\pi r^*}\frac{\widetilde{W}(1)\widetilde{W}(1-h)}{\widetilde{W}(r^*)}\frac{\psi_1(r_<)\psi_2(r_>)}{Q}\,\mathrm{e}^{-\mathrm{i}kx}, \tag{11}$$

with Q being given by (9).

III. Contribution from poles

As described in the previous section and illustrated schematically in Figure 1, the Green's function solution G after Fourier inversion will consist of a sum of residues of poles and an integral around the critical layer branch cut. In this section we investigate the contribution from the poles.

Since the only poles of $G(r;r_0)$ come from zeros of the denominator of (11), there are two possibilities. If $Q = 0$ (implying that $C_1D_2 - C_2D_1 = 0$), then we have a mode in the normal sense, in that both ψ_1 and ψ_2 satisfy both boundary conditions at $r = 0$ and $r = 1$. These poles' contribution to the Fourier integral is (with the contour in the positive sense around the pole)

$$\frac{\omega - U(r^*)k}{2\pi r^*}\frac{\widetilde{W}(1)\widetilde{W}(1-h)}{\widetilde{W}(r^*)}\frac{\psi_1(r_<)\psi_2(r_>)}{\partial Q/\partial k}\,\mathrm{e}^{-\mathrm{i}kx}.$$

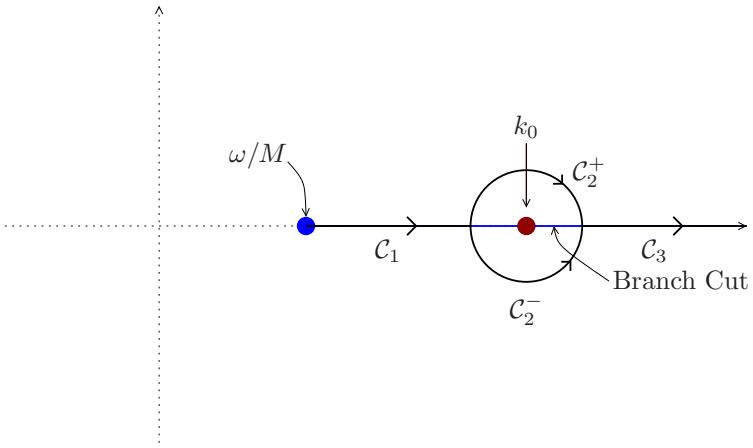

Figure 2. Schematic of the k-plane showing the Fourier inversion contour ($\mathcal{C}_+''$ from figure 1d) collapsed onto the critical layer branch cut. The case $r_0 > 1 - h$ is shown, giving a pole at $k = k_0$ on the branch cut.

Note that the inversion contour goes around poles in the positive sense for $x < 0$ and in the negative sense for $x > 0$.

If the source is in the boundary layer, a second type of singularity is possible for which $\widetilde{W}(r_0) = 0$. Since p_1 and p_2 have been chosen to be linearly independent, this can only happen at a singular point of the Pridmore–Brown equation; i.e. when $r_0 = r_c$. At this point, we find

$$G(r; r_0) = \frac{\psi_1(r_<)\psi_2(r_>)}{C_1 D_2 - C_2 D_1} \left[\frac{-\mathrm{i}\omega k_0}{6\pi(1-r_0)^2 r_0} \left(\frac{1}{k-k_0} + \left(3 - \frac{1}{r_0}\right) \frac{1}{k_0} + O(k-k_0) \right) \right], \tag{12}$$

where

$$k_0 = \frac{\omega h}{(1-r_0)M}, \tag{13}$$

so that there is a pole on the branch cut at $k = k_0$.

The contribution from this pole is less than straightforward to calculate, since it is tied up with the integral around the critical layer branch cut. The integration contour we must use is shown in figure 2 (after having been collapsed onto the branch cut), and the residue of the pole is different below and above the branch cut. The integral required is

$$I = \frac{1}{2\pi} \int_{\mathcal{C}_1 \cup \mathcal{C}_3} \left(G_+(r,k) - G_-(r,k) \right) \mathrm{e}^{-\mathrm{i}kx} \, \mathrm{d}k + \frac{1}{2\pi} \int_{\mathcal{C}_2^+} G_+(r,k) \, \mathrm{e}^{-\mathrm{i}kx} \, \mathrm{d}k - \frac{1}{2\pi} \int_{\mathcal{C}_2^-} G_-(r,k) \, \mathrm{e}^{-\mathrm{i}kx} \, \mathrm{d}k,$$

where $G_+(r,k) = \lim_{\varepsilon \to 0} G(r, k + \mathrm{i}\varepsilon)$ and $G_-(r,k) = \lim_{\varepsilon \to 0} G(r, k - \mathrm{i}\varepsilon)$ are the Greens' function evaluated above and below the branch cut respectively. (In effect, $G_\pm$ is G with $p_2^\pm(r)$ taken in place of $p_2(r)$.) Taking the pole at k_0 given in (12) to be $P_+(r)/(k-k_0)$ evaluated above the branch cut and $P_-(r)/(k-k_0)$ evaluated below the branch cut, we would like to eliminate the $\mathcal{C}_2^\pm$ contours by removing the pole and integrating along the branch cut, yielding

$$I' = \frac{1}{2\pi} \int_{\omega/U}^{\infty} \left(G_+(r,k) - \frac{P_+(r) \, \mathrm{e}^{-\mu(k-k_0)}}{k-k_0} - G_-(r,k) + \frac{P_-(r) \, \mathrm{e}^{-\mu(k-k_0)}}{k-k_0} \right) \mathrm{e}^{-\mathrm{i}kx} \, \mathrm{d}k, \tag{14}$$

where $\mu > 0$ is a positive real constant chosen to maintain the exponential decay of the integrand as $k \to \infty$. The integrals I' and I are related by

$$I = I' + \frac{1}{2\pi} \int_{\mathcal{C}_1 \cup \mathcal{C}_2^- \cup \mathcal{C}_3} \frac{P_+(r) - P_-(r)}{k-k_0} \, \mathrm{e}^{-\mathrm{i}kx - \mu(k-k_0)} \, \mathrm{d}k + \frac{1}{2\pi} \int_{\mathcal{C}_2^+} \frac{P_+(r)}{k-k_0} \, \mathrm{e}^{-\mathrm{i}kx - \mu(k-k_0)} \, \mathrm{d}k - \frac{1}{2\pi} \int_{\mathcal{C}_2^-} \frac{P_+(r)}{k-k_0} \, \mathrm{e}^{-\mathrm{i}kx - \mu(k-k_0)} \, \mathrm{d}k.$$

Since the first integral is exponentially small in the lower half of the k plane as $k \to \infty$ for $x > 0$, and contains no poles other than k_0, we may deform the contour of integration into the lower-half k-plane onto a steepest descent contour. The final two integrals are meromorphic within the region bounded by their contours of integration, and therefore combine to give $-\mathrm{i}P_+(r)\,\mathrm{e}^{-\mathrm{i}k_0 x}$ by the residue theorem. Setting $k = \omega/U + \xi/(\mathrm{i} + \mu/x)$, so that real ξ describes the steepest descent contour, finally yields

$$I = I' - \mathrm{i}P_+(r)\,\mathrm{e}^{-\mathrm{i}k_0 x} + \frac{P_+(r) - P_-(r)}{2\pi}\,\mathrm{e}^{-\mathrm{i}\frac{\omega}{U}x + \mu\left(k_0 - \frac{\omega}{U}\right)}\,E\Big(\mathrm{i}\big(\tfrac{\omega}{U} - k_0\big)(x - \mathrm{i}\mu)\Big), \tag{15}$$

where

$$E(z) = \int_0^\infty \frac{\mathrm{e}^{-t}}{z + t}\,\mathrm{d}t = \mathrm{e}^z\,E_1(z),$$

and E_1 is the exponential integral function [20, §5.1] defined by

$$E_1(z) = \int_z^\infty \frac{\mathrm{e}^{-t}}{t}\,\mathrm{d}t \quad \text{for} \quad |\arg(z)| < \pi \quad \text{and a branch cut along the negative real axis.}$$

Since $E(z) = 1/(z) + O(1/z^2)$ as $z \to \infty$, $I - I'$ is dominated in the far field by the $\mathrm{e}^{-\mathrm{i}k_0 x}$ term which remains $O(1)$ as $x \to \infty$.

Numerically integrating $E(z)$ is relatively easy due to the exponential non-oscillatory decay of the integrand for real x (and indeed E_1 is a standard special function). Evaluating the remaining integral I' is computationally more expensive but otherwise poses no major difficulty.

IV. Numerical results

In this section, a number of numerical results are presented to illustrate the method described so far, and to inform the further analytical discussion that follows. Throughout this section we have taken a mean flow Mach number $M = 0.5$ and an impedance of resistance $\mathrm{Re}(Z) = 2$. Whenever relevant, we have investigated stability by a Briggs-Bers analysis [23, 24], with a simple impedance model of Helmholtz Resonator type.

Numerical experiments reveal a downstream propagating instability pole (denoted k_+) in the upper half k plane just above the critical layer branch cut, and another pole (denoted k_-) closely related to the critical layer. The k_- pole is situated below the branch cut for high frequencies, and leaks to the other Riemann sheet for frequencies below a critical value (which depends on the impedance of the boundary and the thickness of the boundary layer). In addition to these, for $r_0 > 1 - h$ there is also the pole k_0 present on the branch cut. A schematic of this situation is shown in Figure 3. It is insightful to compare the order of magnitude of the contributions from these modes, and the integral around the critical layer branch cut. Such a comparison is shown in Figure 4. As can be seen from Figure 4a,f, the branch cut (I') and the k_--field are important individually, and both are of the same order of magnitude as the instability (k_+), but when summed they almost cancel each other out (see Figure 4b). This leads to an important observation: ignoring the critical layer but including the residue of k_- in the modal sum produces serious errors in the total field. Moreover, the sum of the branch cut integral I' and the k_- field is also almost totally cancelled out by the exponential integral $E(\cdot)$ resulting from the removal of the k_0 pole from the branch cut integral, with what remains being strongly localized about the mass source (Figure 4c).

To sum up, we can split the total pressure field into an acoustic part (obtained by summing up the acoustic modes), the field of the branch cut (in which we include any k_- mode, k_0 mode, and I' and $E(\cdot)$ terms) and the contribution of the instability mode k_+. The field of the critical layer comes from integrating along the branch cut and adding the residue of k_-, in case this is not already "captured" in the integral, and we can observe the fast decay of this in Figure 4c. However if the source is in the boundary layer, we have in addition to this the field generated by k_0, which is described in detail in section VI. Not too far downstream, we can see that for certain parameter values, the branch cut (I') and the poles related to it (k_- and k_0) can have a contribution of the order of magnitude of that of the instability pole (Figure 4).

Further on we compare direct numerical integration along the Fourier inversion contour to the solution obtained by summing the contribution from the acoustic poles. The direct numerical integration was performed using a 4th-order-accurate integrator on equally-spaced points. For $x < 0$ the contour was deformed into the upper-half k-plane, and for $x > 0$ into the lower-half k-plane, in order to speed up convergence. This numerical integration includes only the effect of the acoustic poles, and ignores the contribution from the critical layer branch cut.

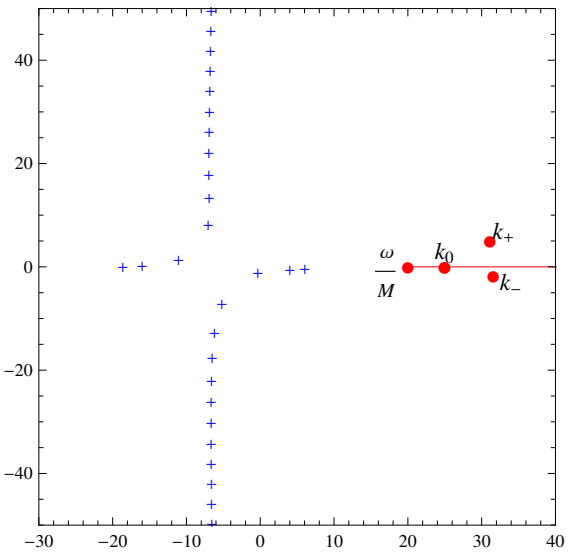

Figure 3. Overview of the k-plane: acoustic poles (+), branch cut (−), branch point ω/M, instability pole k_+, branch-cut-related pole k_- and neutrally unstable pole k_0 (when the source location is in the boundary layer).

For summing the contribution of poles, all poles with $\mathrm{Im}(k) < 400$ were used. This converged rapidly for $x \neq 0$, although the number of poles was insufficient to determine the solution at $x = 0$, as shown by the oscillatory radial behaviour at $x = 0$ in Figure 5. One of the advantages of the modal approach is that it separates modal and non-modal behaviour, and allows us to compare the magnitude of the effect of the critical layer. Besides that, it is stable in the far field for high frequencies (see Figure 5d) and predicts with better accuracy the acoustic field.

It is clear from Figures 5 and 6 that there is an instability mode present. For thicker boundary layers, this instability has a small growth rate (we remark that, in Figure 5a, there is a growth in amplitude upon adding the residue k_+ (iv) to the field in (iii)) and may further turn into a neutrally stable, or possibly decaying mode. When the source is in the boundary layer, the instability is immediately excited, as for a vortex sheet Helmholtz instability from a trailing edge. When the source is outside the boundary layer, the excitation is moved further downstream (see Figure 6c), as for a free vortex sheet [25–27].

The critical layer is negligible when the source is in the mean flow, the pressure field being almost equivalent to that in a uniform flow with Ingard–Myers boundary condition [28, 29] (see Eq. (10) and Figure 7). However, the critical layer becomes important when the source is in the boundary layer, and indeed it is obviously dominant in Figure 6b where all the acoustic modes are cut-off.

V. Asymptotic evaluation of the branch cut contribution

In this section, we aim to make further analytical predictions about the contribution to the overall Green's function from the branch cut. For example, we aim to explain why such significant cancellation was seen in Figure 4 between the contribution from the branch cut (I') and the residue of the k_- pole.

The contribution of the branch cut is seen by taking the large x limit of the Fourier inversion integral around it, while subtracting the residue of the k_0 pole if the source is in the boundary layer. For $r_0 < 1 - h$, this integral is

$$I = \frac{1}{2\pi} \int_{\omega/M}^{\infty} \left(G_+(r,k) - G_-(r,k) \right) \mathrm{e}^{-\mathrm{i}kx} \, \mathrm{d}k, \tag{16}$$

and is given by (14) for $r_0 > 1 - h$. In the large x limit, we may therefore deform the integration contour into the steepest descent contour $k = \omega/M - \mathrm{i}\xi$ with $\xi > 0$, and then apply Watson's lemma to obtain the asymptotic behaviour of this integral. However, in deforming the contour we must be careful not to allow the contour to cross any poles. Figure 8 shows an example of such a deformation. The k_- pole, being below the branch cut, is only a pole of G_- in (16). The pole contribution from integrating around this pole is

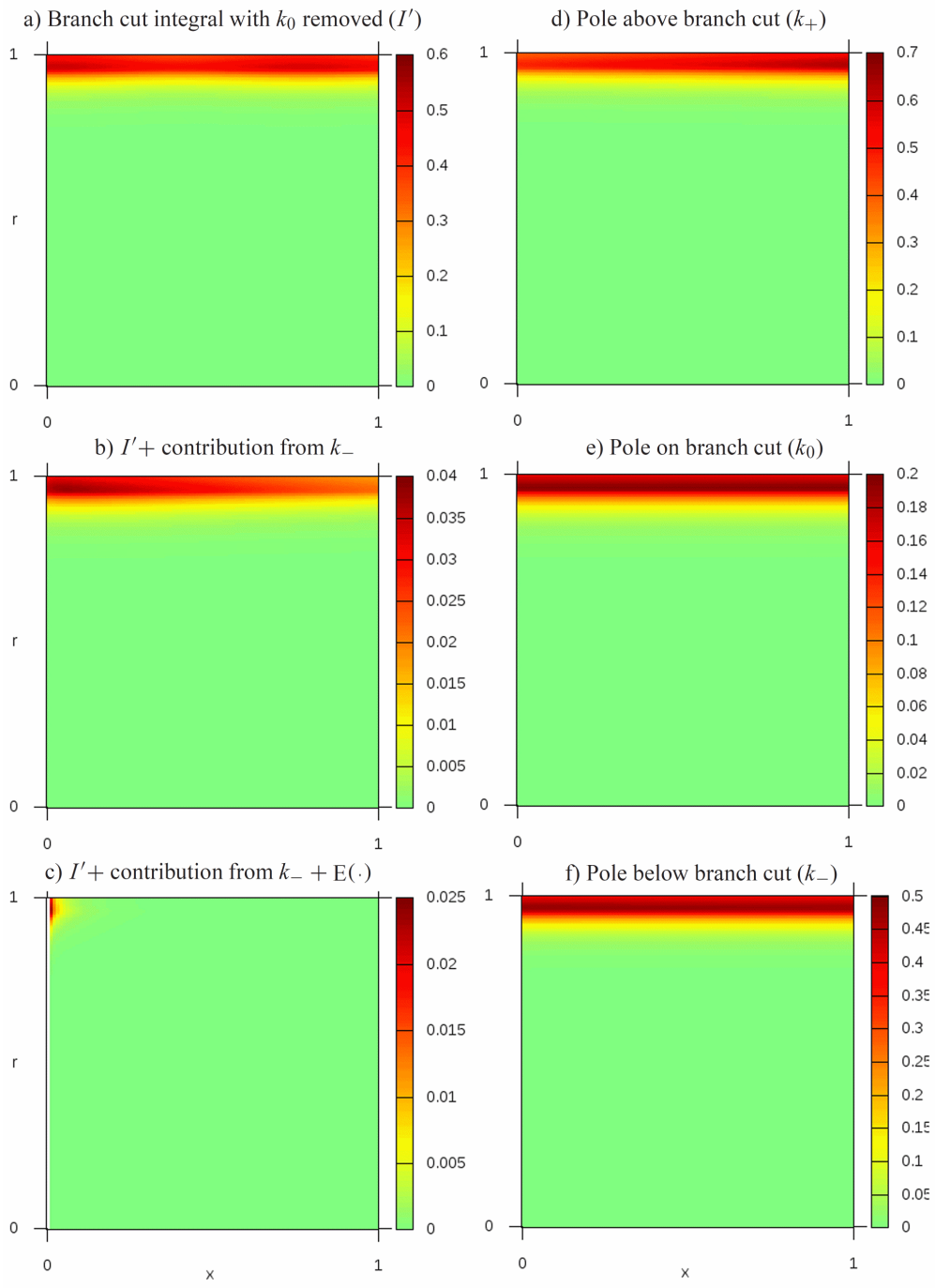

Figure 4. Comparison of the five different contributions to the Greens function from around the branch cut: a) the integral around the branch cut with the k_0-pole removed (I'); b) figure a + the pole below the branch cut; c) figure b + the $E(\cdot)$ term in (15) due to the integral around the branch cut of the pole removal terms. d) the pole above the branch cut; e) the k_0-pole on the branch cut; f) the pole below the branch cut in isolation. The plots are of $|G(x,r)|$, with different scales as shown beside each plot ($Z = 2 + \mathrm{i}$, $\omega = 10$, $h = 0.05$, $r_0 = 0.96$).

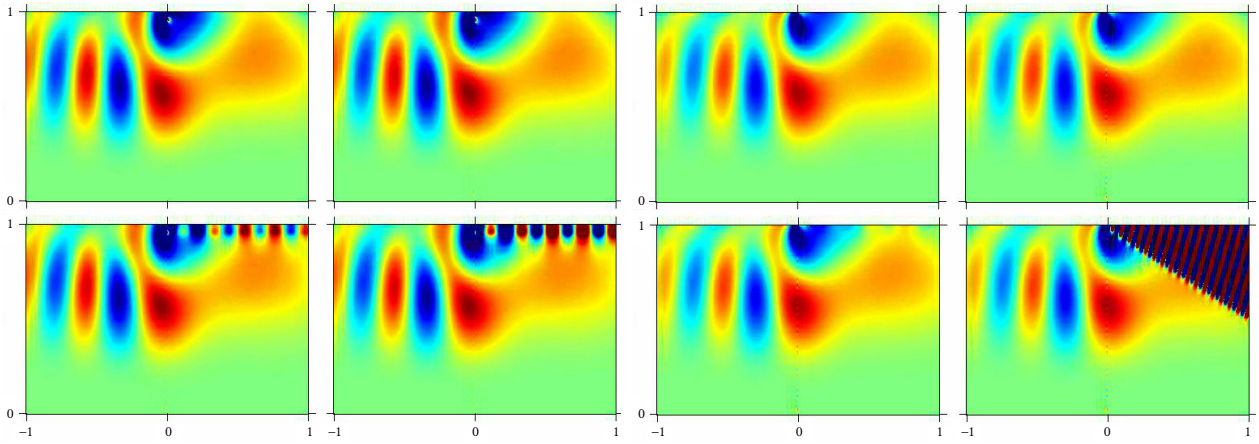

(a) $\omega = 10$, $m = 5$, $Z = 2 - \mathrm{i}$, $h = 0.05$, $r_0 = 0.96$.

(b) $\omega = 10$, $m = 5$, $Z = 2 - \mathrm{i}$, $h = 0.001$, $r_0 = 0.9992$

(c) $\omega = 10$, $m = 24$, $Z = 2 - \mathrm{i}$, $h = 0.001$, $r_0 = 0.9992$

(d) $\omega = 50$, $m = 24$, $Z = 2 + \mathrm{i}$, $h = 0.001$, $r_0 = 0.9992$

Figure 5. The pressure field in (x, r) plane computed by (in the order L-R 1st line, L-R 2nd line): (i) direct numerical Fourier inversion (ignoring the branch cut contribution); (ii) summing the acoustic poles; (iii) summing the acoustic poles and adding the branch cut integrals and k_0 and k_- poles; (iv) summing all contributions ((iii) plus the hydrodynamic pole k_+).

therefore the negative of the pole contribution from k_- in the modal sum of all downstream-propagating modes, and therefore the two exactly cancel. In effect, this deformation of the branch cut contour onto the steepest descent contour removes the k_- pole from the modal sum.

We hypothesize that there are no poles of G_+ that are crossed in this contour deformation, since such poles would necessarily lead to a discontinuous solution in r. We are therefore left with just the integral along the steepest descent contour, which we then expect to be significantly smaller in magnitude than the integral along the critical layer branch cut; this expectation is formalized below. In the case $r_0 > 1 - h$, the integral I consists of a pole contribution from G_+ at $k = k_0$ but otherwise the pole-removal as in (14) is not necessary when we deform the contour to the steepest descent (SD) contour. So we have

$$I = \frac{1}{2\pi} \int_{SD} \left(G_+(r,k) - G_-(r,k)\right) \mathrm{e}^{-\mathrm{i}kx} \, \mathrm{d}k - \mathrm{i}P_+(r) \, \mathrm{e}^{-\mathrm{i}k_0 x},$$

The result is the same as for the $r_0 < 1 - h$ case with the addition of the pole at $k = k_0$.

In conclusion, the contribution from any poles below the branch cut, together with the integral along the branch cut itself, consists of the pole contribution at k_0 in the case $r_0 > 1 - h$, and the steepest-descent contribution

$$I_{sd} = \frac{\mathrm{e}^{-\mathrm{i}\omega x/M}}{2\pi\mathrm{i}} \int_0^\infty \left(G_+(r, \omega/M - \mathrm{i}\xi) - G_-(r, \omega/M - \mathrm{i}\xi)\right) \mathrm{e}^{-x\xi} \, \mathrm{d}\xi.$$

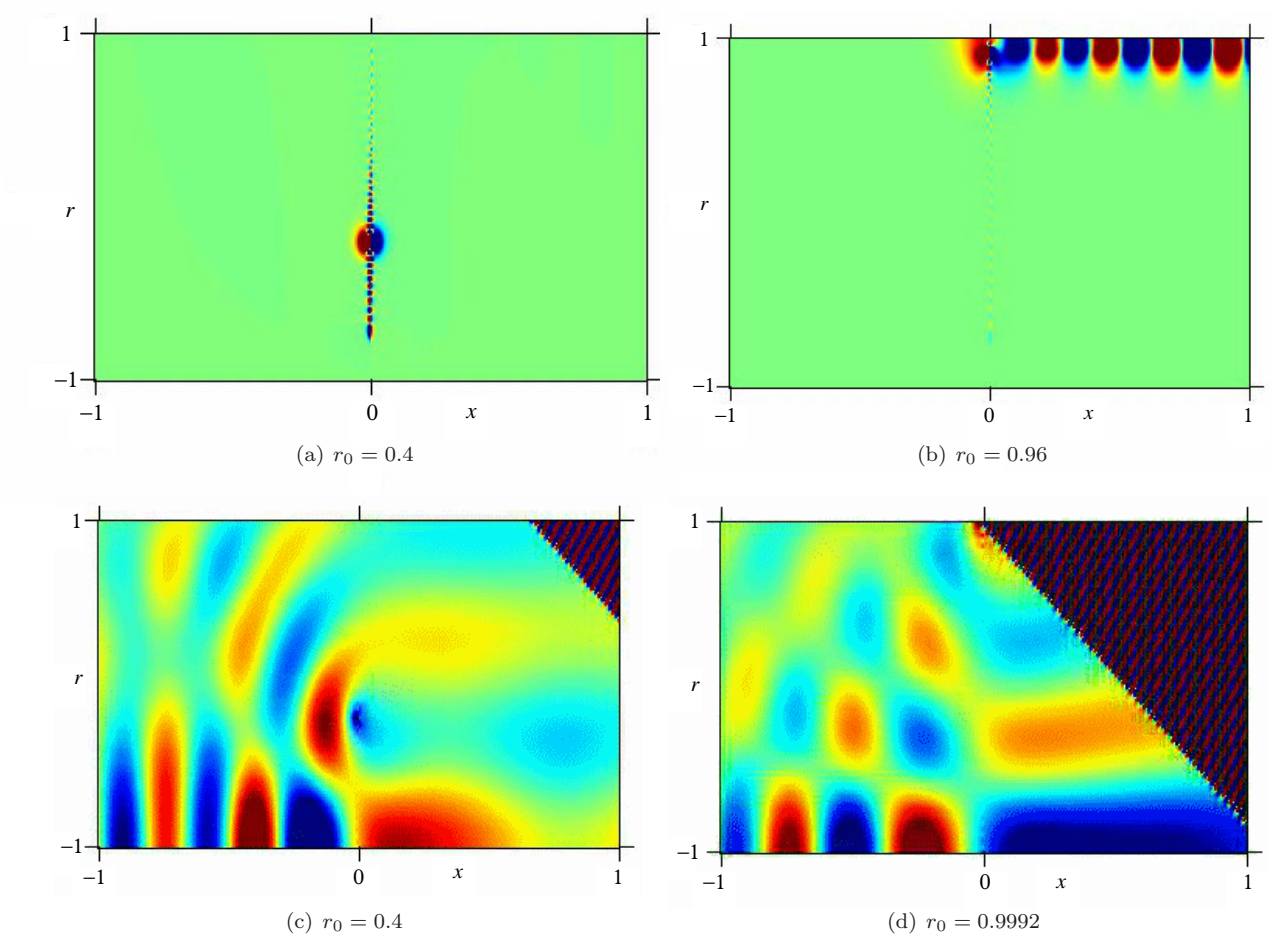

(a) $r_0 = 0.4$ (b) $r_0 = 0.96$

(c) $r_0 = 0.4$ (d) $r_0 = 0.9992$

Figure 6. Total pressure field in (x, r) plane for (a)-(b) $\omega = 10$, $m = 24$, $Z = 2 - \mathrm{i}$, $h = 0.05$; (c)-(d) $\omega = 10$, $m = 0$, $Z = 2 + \mathrm{i}$, $h = 0.001$, and different source locations.

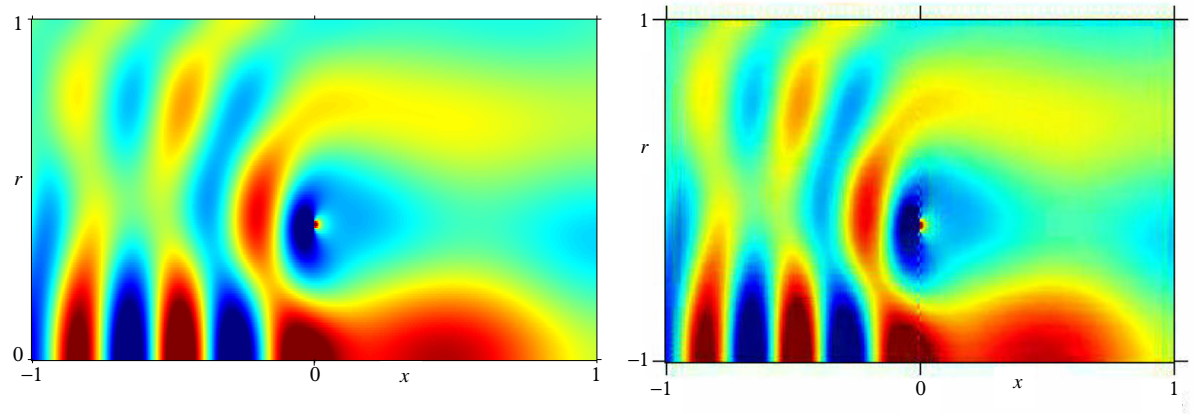

Figure 7. The Green's function with source in mean flow region for (left) uniform flow with Ingard-Myers condition; (right) constant-then-linear flow profile ($\omega = 10, m = 0, Z = 2 - \mathrm{i}, h = 0.001, r_0 = 0.4$.)

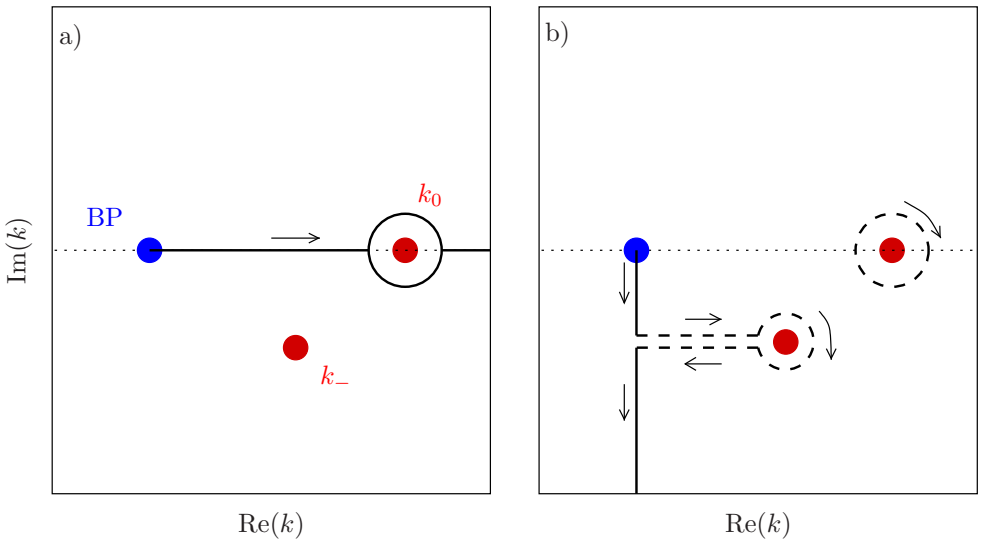

Figure 8. Schematic in the k-plane of: a) the integral along the branch cut from the branch point (labelled BP) to infinity; and b) the same integral deformed onto the steepest descent contour without crossing poles.

If, to leading order for small ξ,

$$G_+(r,\omega/M-\mathrm{i}\xi)-G_-(r,\omega/M-\mathrm{i}\xi)\sim A(r)\xi^\nu+O\big(\xi^{\nu+1}\big) \tag{17}$$

with $\nu>-1$, then Watson's lemma would give, in the large-x limit,

$$I_{sd}\sim\frac{A(r)\Gamma(\nu+1)\,\mathrm{e}^{-\mathrm{i}\omega x/M}}{2\pi\mathrm{i}x^{\nu+1}}+O\big(1/x^{\nu+2}\big);$$

that is, the contribution from the branch cut plus all poles underneath it is an algebraically decaying wave convected with the bulk mean flow (i.e. the phase speed is M), plus, in the case of a point source within the boundary layer $r_0>1-h$, a propagating hydrodynamic wave with wavenumber k_0.

Preliminary calculations indicate that, for both the source and observer in the main flow (i.e. $r_0<1-h$ and $r<1-h$), Eq. (17) does indeed hold with $\nu=3$. Not only does this suggest decay of $O(1/x^4)$, but we also find that, making suitable assumptions about the magnitudes of h and ω, the prefactor $A(r)=O(h^2M^6/\omega^5)$ is typically tiny. For the source within the boundary layer, the decay appears to follow an even higher rate of $O(1/x^5)$. Since these predictions differ from those of Swinbanks[10], work is ongoing to verify them against numerical calculations and to locate the reason for the discrepancy with Swinbanks.

VI. The trailing vorticity field behind a point source in incompressible linear shear flow

The field due to the pole $k=k_0$ is really of hydrodynamical nature, as it remains qualitatively the same in the incompressible limit. By means of an elementary, quintessential model of the field of a line source in simple shear flow, we will show that this field of the pole k_0 is really the trailing vorticity of the source.

The present solution seems to be new, in spite of its rather basic configuration. The nearest solution we found is the velocity field given by Criminale & Drazin [21] for the initial value problem of an impulsive point source in a linear shear layer. Therefore, we will give the solution in detail. First we will Fourier transform in x, similar to the solution of the acoustic problem of the rest of the paper. Here, however, due the simplifications of the model (2D, incompressible) we will have to deal with not normally convergent integrals which have to be considered as integrals of generalised functions.

Next to the free field situation, we will also consider the same problem but with an impedance wall, where the mean flow vanishes at the wall (although in less detailed). This problem is in many aspects similar (there is again the vorticity trailing from the source) but at the same time the interaction with the wall is more subtle. For certain values of the parameters a surface wave exists that may be an instability. Further research is underway.

A. In free field

Consider the 2D model problem of perturbations of a linear sheared mean flow, due to a point source in $x = y = 0$, described after Fourier transformation in x by the following set of equations (in dimensional quantities).

$$\begin{aligned} \frac{\mathrm{i}\Omega}{c_0^2}\tilde{p} - \mathrm{i}k\rho_0\tilde{u} + \rho_0\tilde{v}' &= \rho_0 S\delta(y), \\ \mathrm{i}\rho_0\Omega\tilde{u} + \rho_0 U'\tilde{v} - \mathrm{i}k\tilde{p} &= 0, \\ \mathrm{i}\rho_0\Omega\tilde{v} + \tilde{p}' &= 0, \end{aligned} \tag{18}$$

where $\Omega = \omega - kU$. This system may be further reduced to a form of the Pridmore-Brown equation by eliminating $\tilde{v}$ and $\tilde{u}$, which, upon considering the incompressible limit in a doubly-infinite linear shear flow with $U(y) = U_0 + \sigma y$ (note that σ has the dimension of frequency), becomes

$$\tilde{p}'' + \frac{2k\sigma}{\Omega}\tilde{p}' - k^2\tilde{p} = -\mathrm{i}\rho_0 S\Omega_0\delta(y).$$

The homogeneous equation has two independent solutions $\mathrm{e}^{\pm ky}(\Omega \pm \sigma)$, or

$$\begin{aligned} \tilde{p}_1(y) &= \mathrm{e}^{|k|y}(\Omega + \mathrm{sign}(\mathrm{Re}\, k)\sigma) \\ \tilde{p}_2(y) &= \mathrm{e}^{-|k|y}(\Omega - \mathrm{sign}(\mathrm{Re}\, k)\sigma) \end{aligned}$$

where $|k| = \mathrm{sign}(\mathrm{Re}\, k)k = \sqrt{k^2}$. (Note that neither of these solutions has a log-like singularity or requires a branch cut in the complex-y plane[a].) The Wronskian is

$$W(y;k) = \tilde{p}_2'(y)\tilde{p}_1(y) - \tilde{p}_1'(y)\tilde{p}_2(y) = -2|k|\Omega^2,$$

and the Green's function

$$\tilde{p}(y,k) = \frac{\frac{1}{2}\mathrm{i}\rho_0 S}{|k|\Omega_0}\,\mathrm{e}^{-|ky|}\big(\Omega\Omega_0 - \sigma^2|ky| - \sigma^2\big).$$

The physical field in the x, y-domain is hence obtained by inverse Fourier transformation

$$p(x,y) = \frac{1}{2\pi}\int_{-\infty}^{\infty}\tilde{p}(y,k)\,\mathrm{e}^{-\mathrm{i}kx}\,\mathrm{d}k = \frac{\mathrm{i}\rho_0 S}{4\pi}\int_{-\infty}^{\infty}\frac{\mathrm{e}^{-\mathrm{i}kx-|ky|}}{|k|\Omega_0}\big(\Omega\Omega_0 - \sigma^2|ky| - \sigma^2\big)\,\mathrm{d}k,$$

which has singularities at $k = 0$ (if $\omega^2 \neq \sigma^2$) and at $k = k_0 = \omega/U_0$ from $\Omega_0 = -U_0(k - k_0) = 0$, which is indeed the equivalent of (13) in the duct problem (see below). To study the trailing vorticity we are mainly interested in the contribution of the pole k_0, which is the downstream hydrodynamic wave part of

$$p(x,y) = \frac{\rho_0 S}{2\omega}\sigma^2 H(x)(1 + k_0|y|)\,\mathrm{e}^{-\mathrm{i}k_0 x - k_0|y|} + \frac{\mathrm{i}\rho_0 S}{2\pi}\int_0^{\infty}\frac{\mathrm{e}^{-\lambda|x|}}{\lambda\Omega_0^{\pm}}\left[\big(\Omega^{\pm}\Omega_0^{\pm} - \sigma^2\big)\cos\lambda y - \sigma^2\lambda y\sin\lambda y\right]\mathrm{d}\lambda$$

where $\Omega^{\pm} = \omega \pm \mathrm{i}\lambda U$, $\pm = \mathrm{sign}(x)$, $H(x)$ is Heaviside's step function, and we used the fact that $\cos z$ and $z\sin z$ are even functions.

The singularity at $k = 0$, on the other hand, is not a pole and has a different origin. Due to this singularity the inverse Fourier representation of the pressure is too singular to be interpreted normally. This results – in this 2D incompressible model – from p being not Fourier transformable, not because p itself is singular. As it turns out, p diverges as $\sim \log(x^2 + y^2)$ for $x^2 + y^2 \to \infty$ and hence is not integrable. When we consider the incompressible problem as an inner problem of a larger compressible problem, this diverging behaviour changes in the far field into an outward radiating acoustic wave of some kind.

The inverse Fourier integral, however, can be found if the singular integral is interpreted in the generalised sense, and the singular part is split off. Following [22, p.105], we define the generalised function

$$\lambda^{-1}H(\lambda) = \frac{\mathrm{d}}{\mathrm{d}\lambda}H(\lambda)\log|\lambda|$$

[a]This is as predicted by (2), since there is no curvature term ($1/r_c$ in Eq. 2), the density is constant and the shear is linear.

and integrate by parts to obtain the convergent integrals

$$p(x,y) = \frac{\rho_0 S}{2\omega}\sigma^2 H(x)(1+k_0|y|)\,\mathrm{e}^{-\mathrm{i}k_0 x - k_0|y|} - \frac{\mathrm{i}\rho_0 S}{2\pi}\int_0^\infty \log\lambda \frac{\mathrm{d}}{\mathrm{d}\lambda}\left[\mathrm{e}^{-\lambda|x|}\,\Omega^\pm \cos\lambda y\right]\mathrm{d}\lambda \\ + \frac{\mathrm{i}\rho_0 S}{2\pi}\sigma^2\int_0^\infty \log\lambda\frac{\mathrm{d}}{\mathrm{d}\lambda}\left[\mathrm{e}^{-\lambda|x|}\,\frac{\cos\lambda y + \lambda y\sin\lambda y}{\Omega_0^\pm}\right]\mathrm{d}\lambda$$

Each one can be integrated as follows

$$\int_0^\infty \log\lambda\frac{\mathrm{d}}{\mathrm{d}\lambda}\left[\mathrm{e}^{-\lambda|x|}\,\Omega^\pm\cos\lambda y\right]\mathrm{d}\lambda = \omega\gamma + \tfrac{1}{2}\omega\log(x^2+y^2) - \mathrm{i}U\frac{x}{x^2+y^2}$$

$$\omega\int_0^\infty \log\lambda\frac{\mathrm{d}}{\mathrm{d}\lambda}\left[\mathrm{e}^{-\lambda|x|}\,\frac{\cos\lambda y+\lambda y\sin\lambda y}{\Omega_0^\pm}\right]\mathrm{d}\lambda = \gamma + \tfrac{1}{2}\log(x^2+y^2) \\ + \tfrac{1}{2}(1+k_0 y)E(-\mathrm{i}k_0 x - k_0 y) + \tfrac{1}{2}(1-k_0 y)E(-\mathrm{i}k_0 x + k_0 y)$$

where $\gamma = 0.5772156649\ldots$ is Euler's constant. We have then altogether

$$p(x,y) = -\rho_0 U_0^2\frac{S}{2\pi\omega}(1+k_1 y)\frac{k_0 x}{x^2+y^2} - \mathrm{i}\rho_0 U_0^2\frac{S}{2\pi\omega}(k_0^2-k_1^2)\left(\gamma - \log k_0 + \tfrac{1}{2}\log(k_0^2x^2+k_0^2y^2)\right)$$

$$+\mathrm{i}\rho_0 U_0^2\frac{S}{4\pi\omega}k_1^2\Big[-2\pi\mathrm{i}H(x)\big(1+k_0|y|\big)\,\mathrm{e}^{-\mathrm{i}k_0x-k_0|y|} + (1-k_0y)E(-\mathrm{i}k_0x+k_0y) + (1+k_0y)E(-\mathrm{i}k_0x-k_0y)\Big]$$

Note that the constant term (with $\gamma - \log k_0$) is a result of the generalised integral but is otherwise physically not relevant because only ∇p is defined by the problem. Any additive constant should be determined from matching with a compressible outer field.

As opposed to p, the integrals for v or u are convergent (outside the source) and can be found without resorting to generalised functions. We have

$$\tilde{v}(y,k) = \tfrac{1}{2}S\,\mathrm{e}^{-|ky|}\left(\operatorname{sign}(y) + \operatorname{sign}(\operatorname{Re}k)\frac{\sigma}{\Omega_0}\right)$$

$$\tilde{u}(y,k) = \tfrac{1}{2}\mathrm{i}S\,\mathrm{e}^{-|ky|}\left(\operatorname{sign}(\operatorname{Re}k) + \operatorname{sign}(y)\frac{\sigma}{\Omega_0}\right)$$

and obtain, with $k_1 = \sigma/U_0$,

$$v(x,y) = \frac{S}{2\pi}\int_0^\infty \mathrm{e}^{-\lambda|x|}\sin\lambda y\,\mathrm{d}\lambda + \tfrac{1}{2}\mathrm{i}Sk_1H(x)\,\mathrm{e}^{-k_0|y|-\mathrm{i}k_0x} - \frac{S}{2\pi}k_1\int_0^\infty\frac{\mathrm{e}^{-\lambda|x|}\cos\lambda y}{\lambda\mp\mathrm{i}k_0}\,\mathrm{d}\lambda$$
$$= \frac{S}{2\pi}\frac{y}{x^2+y^2} + \frac{S}{4\pi}k_1\big[2\pi\mathrm{i}H(x)\,\mathrm{e}^{-\mathrm{i}k_0x-k_0|y|} - E(-\mathrm{i}k_0x+k_0y) - E(-\mathrm{i}k_0x-k_0y)\big]$$

$$u(x,y) = \pm\frac{S}{2\pi}\int_0^\infty \mathrm{e}^{-\lambda|x|}\cos\lambda y\,\mathrm{d}\lambda - \tfrac{1}{2}Sk_1H(x)\operatorname{sign}(y)\,\mathrm{e}^{-\mathrm{i}k_0x-k_0|y|} \pm\frac{S}{2\pi}k_1\int_0^\infty\frac{\mathrm{e}^{-\lambda|x|}\sin\lambda y}{\lambda\mp\mathrm{i}k_0}\,\mathrm{d}\lambda$$
$$= \frac{S}{2\pi}\frac{x}{x^2+y^2} + \mathrm{i}\frac{S}{4\pi}k_1\big[2\pi\mathrm{i}H(x)\operatorname{sign}(y)\,\mathrm{e}^{-\mathrm{i}k_0x-k_0|y|} + E(-\mathrm{i}k_0x+k_0y) - E(-\mathrm{i}k_0x-k_0y)\big]$$

Note that the branch cuts of the exponential integrals (in the E-functions) cancel the jumps due to the $H(x)$-terms, to produce continuous p and v fields. Only u has a tangential discontinuity along $y=0, x>0$ due to the $\operatorname{sign}(y)$-term. This corresponds to the $\delta(y)$-function behaviour of the vorticity mentioned in Appendix A.

A graphical example of this solution is given in figure 9.

For the comparison with the acoustic problem, we note that in the shear layer of the circular duct we have

$$U(r) = \frac{M}{h}(1-r) = \frac{M}{h}(1-r_0) + \frac{M}{h}(r_0-r))$$

which is equivalent to the 2D problem if we identify $y = a(r_0-r)$, $U_0 = c_0M(1-r_0)/h$, and $\sigma = c_0M/ah$ and $\omega := \omega c_0/a$, such that the dimensionless duct equivalent of k_0 and k_1 are

$$k_0 := k_0 a = \frac{a\omega}{U_0} = \frac{\omega h}{M(1-r_0)}, \quad k_1 := k_1 a = \frac{1}{1-r_0}.$$

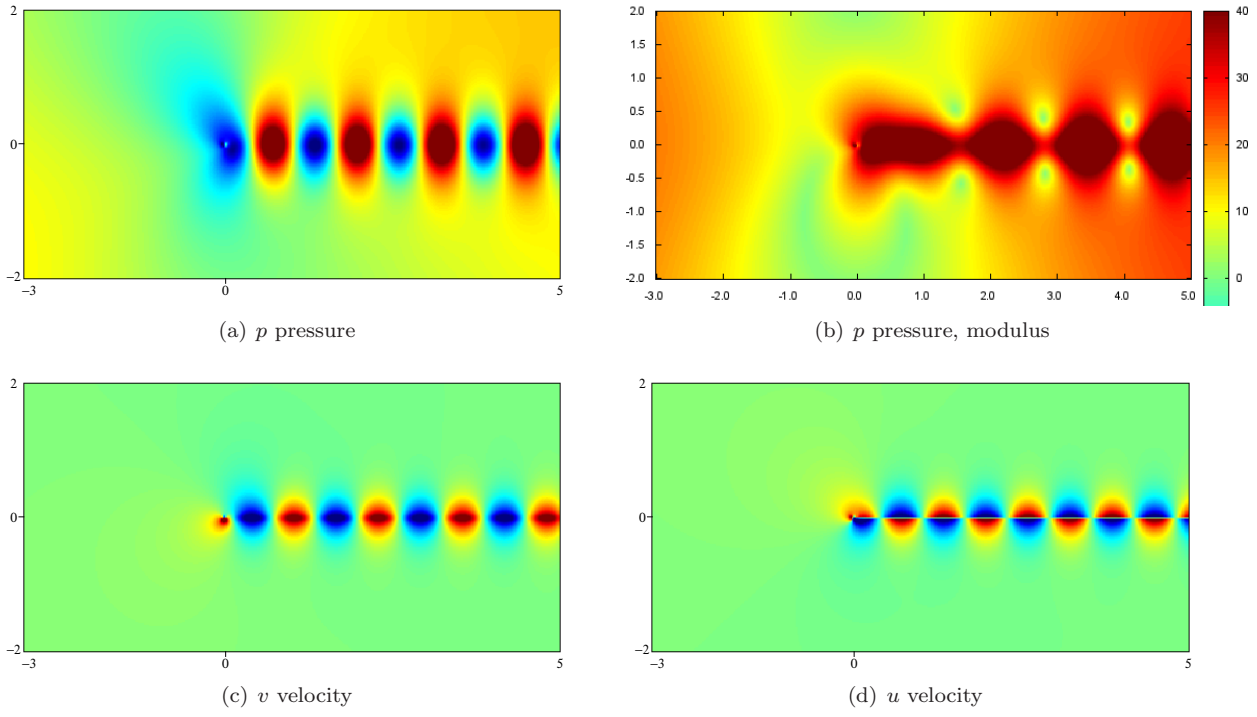

(a) p pressure

(b) p pressure, modulus

(c) v velocity

(d) u velocity

Figure 9. Pressure and velocity field of line source in incompressible linear mean shear flow for $\omega = 10$, $\sigma = 20$ and $U_0 = 2$, $x \in [-3, 5]$.

B. Near an impedance wall

Consider the same equations (18) as before, but now in a region $y \in [0, \infty)$, with a source at $y = y_0$, and an impedance wall at $y = 0$. We have with $\Omega = \omega - kU$, $U(y) = U_0 + \sigma(y - y_0)$, $U_0 = \sigma y_0$, $\Omega_0 = \omega - kU_0$, $k_0 = \omega/U_0$ and $\tilde{p}(0) = -\rho_0 U_0 \zeta \tilde{v}(0)$ at $y = 0$, the Pridmore-Brown-type equation

$$\tilde{p}'' + \frac{2k\sigma}{\Omega}\tilde{p}' - k^2\tilde{p} = -\mathrm{i}\rho_0 S\Omega_0\delta(y - y_0).$$

with

$$\mathrm{i}k_0\tilde{p}(0) = \zeta\tilde{p}'(0).$$

Similarly to the free field configuration, the solution can be constructed and is found to be

$$p = \frac{\mathrm{i}\rho_0 S}{2|k|\Omega_0}\,\mathrm{e}^{-|k|y_>}(\Omega_> - \operatorname{sign}(\operatorname{Re} k)\sigma)\cdot \\ \cdot\left(\mathrm{e}^{|k|y_<}(\Omega_< + \operatorname{sign}(\operatorname{Re} k)\sigma) + \frac{k - \mathrm{i}\zeta^{-1}(k_1 + \operatorname{sign}(\operatorname{Re} k)k_0)}{k - \mathrm{i}\zeta^{-1}(k_1 - \operatorname{sign}(\operatorname{Re} k)k_0)}\,\mathrm{e}^{-|k|y_<}(\Omega_< - \operatorname{sign}(\operatorname{Re} k)\sigma)\right)$$

where $y_< = \min(y, y_0)$, $y_> = \max(y, y_0)$, $\Omega_{<>} = \Omega(y_{<>})$, and $k_1 = \sigma/U_0$.

Again, the physical field in the x, y-domain is obtained by inverse Fourier transformation,

$$p(x, y) = \frac{1}{2\pi}\int_{-\infty}^{\infty}\tilde{p}(y, k)\,\mathrm{e}^{-\mathrm{i}kx}\,\mathrm{d}k$$

with a pole at $k = k_0$ (yielding the vorticity shed from the source), and, for certain parameter values, at

$$k = k_2 = \frac{\mathrm{i}}{\zeta}(k_1 - \operatorname{sign}(\operatorname{Re} k_2)k_0) = \frac{\operatorname{Im}\zeta + \mathrm{i}\operatorname{Re}\zeta}{|\zeta|^2}\frac{\sigma - \operatorname{sign}(\operatorname{Re} k_2)\omega}{U_0}.$$

This pole must have a counterpart in the compressible 3D problem, but due to time constraints we have not finished this analysis yet. Further research is underway.

VII. Conclusions

The Green's function for a mass source in a cylindrical duct with constant mean flow and a linear-shear boundary layer of thickness h has been given, with no restriction on h being either small or large. In sheared flow, there are three possible contributions to the pressure field, being acoustic modes, surface modes [30,31], and the critical layer branch cut (or, as it is sometimes called, the continuous spectrum). The first two occur as poles of the Green's function, the only difficult question in these cases being whether modes should be considered to be left-running (present for $x < 0$) or right-running (present for $x > 0$), which may be ascertained by applying the Briggs–Bers criterion [23, 24]. One of the reasons for this paper was to address the third problem: that of the critical layer branch cut.

The continuous spectrum, through a Briggs–Bers analysis, is found to only take effect downstream of the point forcing and contributes to the critical layer in five ways:

1. through the pole just above the branch cut (k_+);
2. through the pole just below or behind the branch cut (k_-);
3. through the integral along the branch cut, with possible pole at k_0 removed (the pole being present for a point forcing within the boundary layer, $r_0 > 1 - h$);
4. if $r_0 > 1 - h$, through the pole at $k = k_0$; and
5. if $r_0 > 1 - h$, through the exponential integral $E(\cdot)$ in (15).

If, as hypothesized in section V, there are no poles of G_+ in the lower-half k-plane below the branch cut (or, in other words, if there are no modes hiding behind the critical layer branch cut in the lower-half k-plane with $\mathrm{Re}(k) > \omega/U$), then the contributions from 2, 3 and 5 almost totally cancel and decay algebraically away from $x = 0$ (determined here to be as $1/x^4$ if $r_0 < 1 - h$). If there are such poles, they would add a residue contribution in the same way as for the acoustic and surface modes, and this contribution would necessarily be discontinuous in r and necessarily decay exponentially downstream. Note that either of 2 or 3 themselves may give rather a large contribution, so that, for instance, including the k_- pole below the branch cut but ignoring the branch cut itself would give significantly inaccurate results. The dominant effect of the branch cut is due to the poles either just above or on it, with the pole k_0 being present for $r_0 > 1 - h$. Of these, the k_+ pole just above the branch cut is (in all cases considered here) a convective instability that dominates far downstream of the forcing point, while the pole on the branch cut (if present) is a neutrally-stable propagating mode, with a phase velocity equal to the velocity of the mean flow. The field due to latter is the trailing vorticity of the source and is of hydrodynamical nature, remaining qualitatively the same in the incompressible limit.

Appendix

A. An investigation on the type of source

Since some of the results presented in this paper depend essentially on the type of source assumed, in this appendix we investigate the type of source in further detail.

Consider the equations for conservation of mass and momentum with a mass source Q and an external force $\boldsymbol{F}$. By first principle arguments [32] of integral balance of mass and linear momentum in inviscid flow, we obtain

$$\frac{\partial \rho}{\partial t} + \nabla\cdot(\rho \boldsymbol{v}) = Q$$
$$\frac{\partial \rho \boldsymbol{v}}{\partial t} + \nabla\cdot(\rho \boldsymbol{v}\boldsymbol{v}) + \nabla p = \boldsymbol{F} + Q\boldsymbol{v}.$$

Note that the issuing mass adds momentum by an amount of $Q\boldsymbol{v}$. The momentum equation contains the left-hand-side of the mass equation and is in the usual way reduced to

$$\rho \frac{\partial \boldsymbol{v}}{\partial t} + \rho(\boldsymbol{v}\cdot\nabla)\boldsymbol{v} + \nabla p = \boldsymbol{F}.$$

In the model studied here, we assume only a mass source Q and no body force, i.e. $\boldsymbol{F} = 0$. However, in general the presence of a mass source in a mean flow may disturb the flow such that an associated force is to be included, for example to model effects of turbulence, viscosity, separation or vortex shedding. In order to sketch the effect of this we consider a combination of a time-harmonic line point mass source and a line point force in a mean flow of linear shear. (A line source is relevant because in our duct problem the point source is broken up into a Fourier sum of circular line sources.) We have for the effectively 2D problem

$$\rho = \rho_0 + c_0^{-2} p\, \mathrm{e}^{\mathrm{i}\omega t},\ \boldsymbol{v} = (U(y) + u\, \mathrm{e}^{\mathrm{i}\omega t}, v\, \mathrm{e}^{\mathrm{i}\omega t}),\ p = p_0 + p\, \mathrm{e}^{\mathrm{i}\omega t},\ Q = q\, \mathrm{e}^{\mathrm{i}\omega t},\ \boldsymbol{F} = (f, g)\, \mathrm{e}^{\mathrm{i}\omega t}$$

$$\begin{aligned} \frac{1}{c_0^2}\left(\mathrm{i}\omega + U\frac{\partial}{\partial x}\right) p + \rho_0 \left(\frac{\partial u}{\partial x} + \frac{\partial v}{\partial y}\right) &= q \\ \rho_0 \left(\mathrm{i}\omega + U\frac{\partial}{\partial x}\right) u + \rho_0 \frac{\mathrm{d}U}{\mathrm{d}y} v + \frac{\partial p}{\partial x} &= f \\ \rho_0 \left(\mathrm{i}\omega + U\frac{\partial}{\partial x}\right) v + \frac{\partial p}{\partial y} &= g \end{aligned}$$

When we split up the velocity in a solenoidal and a vortical part

$$u = \frac{\partial \phi}{\partial x} + \frac{\partial \psi}{\partial y}, \quad v = \frac{\partial \phi}{\partial y} - \frac{\partial \psi}{\partial x}, \quad \chi = \frac{\partial v}{\partial x} - \frac{\partial u}{\partial y} = -\nabla^2 \psi,$$

where χ is the (z-component of) the vorticity, and assume the mean flow being given by

$$U(y) = U_0 + \sigma y$$

we obtain after taking the curl of the momentum equation

$$\begin{aligned} \frac{1}{c_0^2}\left(\mathrm{i}\omega + U\frac{\partial}{\partial x}\right) p + \rho_0 \nabla^2 \phi &= q, \\ \rho_0 \left(\mathrm{i}\omega + U\frac{\partial}{\partial x}\right) \left(\chi + \frac{\sigma}{\rho_0 c_0^2} p\right) &= \sigma q - \frac{\partial f}{\partial y} + \frac{\partial g}{\partial x}. \end{aligned}$$

Consider a point source and point force

$$q = \rho_0 S \delta(x)\delta(y), \quad (f, g) = \rho_0 U_0 (A, B)\delta(x)\delta(y).$$

to obtain

$$\left(\mathrm{i}\omega + U\frac{\partial}{\partial x}\right) \left(\chi + \frac{\sigma}{\rho_0 c_0^2} p\right) = \sigma S \delta(x)\delta(y) - A U_0 \delta(x)\delta'(y) + B U_0 \delta'(x)\delta(y)$$

with (causal) solution

$$\begin{aligned} \chi + \frac{\sigma}{\rho_0 c_0^2} p &= (k_1 S - k_1 A - \mathrm{i} k_0 B) H(x)\, \mathrm{e}^{-\mathrm{i}k_0 x}\, \delta(y) - A H(x)\delta'(y) + B\delta(x)\delta(y), \\ k_0 = \frac{\omega}{U_0}, \quad k_1 &= \frac{\sigma}{U_0}, \end{aligned}$$

because $h(x)\delta'(x) = h(0)\delta'(x) - h'(0)\delta(x)$.

We conclude that with $A = B = 0$ an undulating vortex sheet is produced extending behind the point source, which is not unexpected. (Of course, no vorticity is really produced, because the time-averaged χ is zero. It is only a redistribution.) The field with $A, B \neq 0$, on the other hand, is much more singular. Therefore we will choose here no associated force field.

Note that for uniform mean flow ($\sigma = 0$) vorticity is always produced by an external force field (for example at a trailing edge [33]), but not by a pure mass source.

Acknowledgement

M. Darau's contribution was part of PhD work in a cooperation between TU Eindhoven (Netherlands) and the West University of Timisoara (Romania), supervised by professors Robert R.M. Mattheij and Stefan Balint. E.J. Brambley was supported by a Research Fellowship at Gonville & Caius College, Cambridge.

References

[1]S.A. Maslowe, Critical Layers in Shear Flows, *Ann. Rev. Fluid Mech*, 18, p.405–432, 1986

[2]P. Huerre, The Nonlinear Stability of a Free Shear Layer in the Viscous Critical Layer Regime, *Philosophical Transactions of the Royal Society of London. Series A, Mathematical and Physical Sciences* 293(1408), p.643–672, 1980

[3]P. Huerre and J.F. Scott Effects of Critical Layer Structure on the Nonlinear Evolution of Waves in Free Shear Layers, *Proceedings of the Royal Society of London. Series A, Mathematical and Physical Sciences* 371(1747), p.509-524, 1980

[4]L.M.B.C. Campos and P.G.T.A. Serrão, On the Acoustics of an Exponential Boundary Layer, *Philosophical Transactions of the Royal Society of London A* 356, p.2335–2378, 1998

[5]Lord Rayleigh, *The Theory of Sound*, vol.2, Macmillan, 1896

[6]K.M. Case, Stability of inviscid plane Couette flow *Phys. Fluids* 3, p.143–148, 1960

[7]C.K.W. Tam and L. Auriault, The Wave Modes in Ducted Swirling Flows, *Journal of Fluid Mechanics* 371, p.1–20, 1998

[8]C.J. Heaton and N. Peake, Algebraic and Exponential Instability of Inviscid Swirling Flow, *Journal of Fluid Mechanics* 565, p.279–318, 2006

[9]L.M.B.C. Campos and P.G.T.A. Serrão, On the Continuous Spectrum of Sound in Sheared and Swirling Flows, *AIAA paper 2010-4033*, 2010

[10]M.A. Swinbanks, The Sound Field Generated by a Source Distribution in a Long Duct carrying Sheared Flow, *Journal of Sound and Vibration* 40, p.51–76, 1975

[11]M.J. Lighthill An Introduction to Fourier Analysis and Generalised Functions, *Cambridge University Press*, 1958

[12]S. Félix and V. Pagneux, Acoustic and Hydrodynamic Modes Generated by a Point Source in a Duct Carrying a Parallel Shear Flow, *Proceedings of the 19th International Congress on Acoustics*, Madrid, 2-7 September, 2007.

[13]C.J. Brooks and A. McAlpine, Sound Transmission in Ducts with Sheared Mean Flow, *AIAA paper 2007-3545*, 2007.

[14]O. Olivieri, A. McAlpine, and R.J. Astley, Determining the Pressure Modes at High Frequencies in Lined Ducts with a Shear Flow, *AIAA paper 2010-3944*, 2010.

[15]G. Boyer, E. Piot and J.P. Brazier, Theoretical investigation of hydrodynamic surface mode in a lined duct with sheared flow and comparison with experiment, *Journal of Sound and Vibration* 330, 2011, p.1793–1809.

[16]G.G. Vilenski and S.W. Rienstra, On Hydrodynamic and Acoustic Modes in a Ducted Shear Flow with Wall Lining, *Journal of Fluid Mechanics* 583, p.45–70, 2007

[17]S.W. Rienstra and B.J. Tester, An Analytic Green's Function for a Lined Circular Duct Containing Uniform Mean Flow, *Journal of Sound and Vibration* 317, p.994–1016. 2008

[18]D.C. Pridmore-Brown, Sound Propagation in a Fluid Flowing Through an Attenuating Duct, *Journal of Fluid Mechanics* 4, p.393–406, 1958

[19]G.G. Vilenski and S.W. Rienstra, Numerical Study of Acoustic Modes in Ducted Shear Flow, *Journal of Sound and Vibration* 307, p.610–626, 2007

[20]M. Abramowitz and I.A. Stegun, *Handbook of Mathematical Functions*, 9th edition, Dover, 1964

[21]W.O. Criminale and P.G. Drazin, The Evolution of Linearized Parallel Flows, *Studies in Applied Mathematics* 83, p.123–157, 1990

[22]D.S. Jones, *The Theory of Generalised Functions*, 2nd ed., Cambridge University Press, Cambridge, 1982

[23]S.W. Rienstra and M. Darau, Boundary Layer Thickness Effects of the Hydrodynamic Instability along an Impedance Wall, *Journal of Fluid Mechanics* 671, p.559–573, 2011

[24]E.J. Brambley, A well-posed boundary condition for acoustic liners in straight ducts with flow, *AIAA Journal* 49(6), p.1272–1282, 2011

[25]D.S. Jones and J.D. Morgan A Linear Model of a Finite Amplitude Helmholtz Instability, *Proc. R. Soc. London* A.338, p.17–41, 1974

[26]R.M. Munt, Acoustic The Interaction of Sound with a Subsonic Jet Issuing from a Semi-Infinite Cylindrical Pipe, *Journal of Fluid Mechanics* 83, p.609–640, 1977

[27]S.W. Rienstra, On the Acoustical Implications of Vortex Shedding from an Exhaust Pipe, *Journal of Engineering for Industry* 103, p.378–384, 1981

[28]K.U. Ingard, Influence of Fluid Motion Past a Plane Boundary on Sound Reflection, Absorption, and Transmission, *Journal of the Acoustical Society of America* 31, p.1035–1036, 1959

[29]M.K. Myers, On the acoustic boundary condition in the presence of flow, *Journal of Sound and Vibration* 71, p.429–434, 1980

[30]S.W. Rienstra, A Classification of Duct Modes based on Surface Waves, *Wave Motion* 37, p.119–135, 2003

[31]E.J. Brambley and N. Peake, Classification of Aeroacoustically Relevant Surface Modes in Cylindrical Lined Ducts, *Wave Motion* 43, p.301–310, 2006

[32]S.M. Klisch, T.J. Van Dyke and A. Hoger, A Theory of Volumetric Growth for Compressible Elastic Biological Materials *Mathematics and Mechanics of Solids* 6 , p.551–575, 2001

[33]S.W. Rienstra, Sound Diffraction at a Trailing Edge, *Journal of Fluid Mechanics*, 108, p.443–460, 1981